

ARTICLE OPEN



Brain CB2 receptor: a new target in medication development for treating opioid use disorder in rodents

Omar Soler-Cedeño¹, Hai-Ying Zhang², Emma Xiong¹, Guo-Hua Bi¹, Hannah Alton¹, Maia Maras¹, Qing-Rong Liu³, Pinaki Bhattacharjee⁴, Malliga R. Iyer⁴ and Zheng-Xiong Xi¹✉

This is a U.S. Government work and not under copyright protection in the US; foreign copyright protection may apply 2025

Opioid use disorder (OUD) remains a major public health crisis, underscoring the urgent need for safer and more effective treatments. Cannabinoid CB2 receptor (CB2R) agonists show therapeutic promise for neuropsychiatric disorders and pain, with minimal psychoactive effects by themselves, but their potential in treating OUD is not well defined. Here, we report that MRI-2594, a novel, highly selective CB2R agonist, reduced heroin self-administration and heroin-primed reinstatement of drug-seeking behavior in rats. MRI-2594 produced modest analgesia by itself without impairing oxycodone-induced analgesia, hyperlocomotion, or causing sedation. Local infusion of MRI-2594 into the ventral tegmental area (VTA) or nucleus accumbens (NAc) also inhibited heroin self-administration in rats. Systemically administered MRI-2594 reduced dopamine (DA) release in the NAc, as measured by fiber photometry. In DAT-Cre mice, MRI-2594 attenuated brain-stimulation reward driven by optogenetic activation of VTA DA neurons – an effect blocked by the selective CB2R antagonist MRI-2687. To confirm CB2R mechanism, we generated a new strain of CB2-KO-eGFP mice in which the CB2R coding region was replaced with an eGFP reporter. Immunostaining revealed CB2R-driven GFP expression in tyrosine hydroxylase (TH)-positive VTA DA neurons of CB2-KO-eGFP, but not wild-type, mice. Lastly, MRI-2594 inhibited heroin self-administration in wild-type but not CB2-KO-eGFP mice. These findings demonstrate that brain CB2Rs mediate the anti-addictive effects of MRI-2594 and highlight CB2R as a potential target for OUD therapy.

Molecular Psychiatry (2026) 31:2351–2364; <https://doi.org/10.1038/s41380-025-03377-3>

INTRODUCTION

Opioid use disorder (OUD) has emerged as a significant public health crisis, affecting millions worldwide [1]. In the United States alone, overdose deaths exceeded 100,000 in 2021 [2], driven largely by the misuse of fentanyl, its analogs, and prescription opioids such as oxycodone. Approximately 80% of individuals with OUD develop the disorder through the nonmedical use of opioids [3, 4]. Although treatments like methadone and buprenorphine are available, relapse rates remain alarmingly high [5]. These opioid agonists also carry risks of dependence and withdrawal symptoms [5, 6]. Thus, there is an urgent need to develop novel, non-opioid pharmacotherapy that can reduce opioid use, dependence, and overdose risk.

With the ongoing legalization of cannabis in the U.S., cannabinoids have gained attention as potential treatments for OUD. Both cannabinoids and opioids produce therapeutic analgesia [7, 8]; however, cannabinoids generally have better safety profile and lower abuse potential [9, 10]. Previous studies have shown that cannabinoid CB1 receptor (CB1R) antagonists – such as rimonabant, AM4113, PIMSR, and AM6527 – can reduce drug-taking and drug-seeking behaviors [11–15], including heroin self-administration [16] and morphine-induced conditioned place preference (CPP) in rodents [17]. However, rimonabant's clinical

development was halted due to severe psychiatric side effects, including depression and suicidal ideation [13, 18–20].

As an alternative, the brain's cannabinoid CB2 receptor (CB2R) has emerged as a potential target. Unlike CB1R antagonists, CB2R agonists do not produce psychoactive effects [21–23]. Preclinical studies have shown that CB2R agonists reduce self-administration, CPP, and locomotor activation induced by cocaine, nicotine, methamphetamine, and alcohol [16, 24–32]. However, fewer studies have examined the role of CB2R in OUD, though some evidence suggests CB2R activation can attenuate morphine-induced CPP, physical dependence, and tolerance [33–37]. Whether selective CB2R agonists can suppress opioid-taking and -seeking behavior, however, remains unclear.

This study examined whether MRI-2594, a novel and selective CB2R agonist (with a K_i of 0.031 nM and an EC_{50} of 0.09 nM for human CB2R, and >1800-fold selectivity for CB2R over CB1R) [38, 39], can reduce heroin self-administration and relapse-like behavior in rats. We also assessed whether MRI-2594 induces adverse effects such as sedation, motor impairment, or interference with therapeutic opioid analgesia.

We also investigated the role of the mesolimbic dopamine (DA) system in MRI-2594's action. To test this hypothesis, MRI-2594 was administered intranasally and directly into the ventral tegmental

¹Addiction Biology Unit, Molecular Targets and Medications Discovery Branch, Intramural Research Program, National Institute on Drug Abuse, Baltimore, MD 21224, USA.

²Section on Molecular Neuroscience, National Institute on Mental Health, Intramural Research Program, Bethesda, MD 20892, USA. ³Laboratory of Clinical Investigation, National Institute on Aging, Intramural Research Program, Baltimore, MD 21224, USA. ⁴Section on Medicinal Chemistry, National Institute on Alcohol Abuse and Alcoholism, Intramural Research Program, Bethesda, MD 20852, USA. ✉email: zxi@intra.nida.nih.gov

Received: 29 March 2025 Revised: 29 October 2025 Accepted: 27 November 2025

Published online: 11 December 2025

area (VTA) or nucleus accumbens (NAc), followed by heroin self-administration tests. Additionally, we used fiber photometry and optogenetics to assess the effects of MRI-2594 on NAc DA release in WT mice and DA-mediated optical intracranial self-stimulation (oICSS) behavior in DAT-Cre mice.

Given conflicting evidence on CB2R expression in the brain and neurons, we reexamined this issue. Some studies report CB2R expression in midbrain dopamine and glutamate neurons [11, 22, 40, 41], as well as hippocampal glutamate neurons [42, 43]. In contrast, studies using GFP-reporter mouse lines have produced inconsistent results – showing GFP expression in microglia of the healthy mouse brain in one line [44], or only in 5xFAD Alzheimer's disease model mice in another line [45]. A review of the transgenic strategies used in these lines revealed critical limitations. In the CB2-GFPTg BAC transgenic line [44], the green fluorescent protein (GFP) transgene was randomly inserted into mouse genome, which may lead to ectopic rather than endogenous CB2R expression (Supplementary Fig. 1A). In the CB2^{EGFP/f/f} line [45], the GFP cassette was placed in the 3' untranslated region downstream of the CB2R translation stop codon, suggesting that the endogenous CB2R machinery may not drive GFP translation (Supplementary Fig. 1B), resulting in undetectable GFP expression under normal healthy conditions.

To resolve this issue, we generated a novel CB2-KO-eGFP reporter mouse in which the CB2R-coding sequence is replaced by enhanced GFP (eGFP) under native regulatory control (Supplementary Fig. 1C). This mouse serves both as a full CB2R-knockout (CB2-KO) and an eGFP reporter line. Using this line, we observed GFP expression in DA neurons in the VTA and cells in the NAc. Importantly, CB2R deletion abolished MRI-2594's ability to reduce heroin self-administration and intake.

Together, these findings provide compelling evidence supporting that brain CB2Rs play a functional role in regulating opioid-related behaviors and support the further development of CB2R agonists, such as MRI-2594, as potential therapies for OUD.

MATERIALS AND METHODS

Animals

Male Long-Evans rats were used for intravenous (i.v.) drug self-administration and reinstatement test. Male and female DAT-Cre mice bred at the NIDA IRP were used for optical ICSS. Wildtype and CB2-KO-eGFP mice (Ingenious Targeting Laboratory) were used for heroin self-administration and immunohistochemistry (IHC). All animals were housed in a climate-controlled room on a 12 h light/dark cycle. All procedures were approved by the Animal Care and Use Committee of the National Institute on Drug Abuse Intramural Research Program (see more details in SI).

Experiment 1: Intravenous heroin self-administration and reinstatement test in rats

Intravenous catheterization surgery and heroin self-administration procedures were performed as described previously [46, 47]. Briefly, rats were implanted with i.v. catheters in the right jugular vein under ketamine/xylazine anesthesia. Catheters were secured and routed to a head-mounted connector, fixed with screws and dental acrylic. Catheters were flushed daily with gentamicin-heparin-saline (30 IU/ml).

After recovery, rats were trained to self-administer heroin under fixed-ratio (FR1 first, followed by FR2) schedules. Each active lever press delivered a heroin infusion, paired with light-tone cues. There was no time out. Sessions lasted 3 h or ended after 50 infusions. Rats were trained to stable criteria (≥ 15 infusions/session, $< 20\%$ variability across 3 days, active/inactive ratio $> 2:1$).

MRI-2594 (3, 10, or 30 mg/kg, i.p.) or vehicle (5% Cremophor, i.p.) was tested in a between-subjects design during FR2 heroin self-administration. Between tests, animals were returned to daily sessions until baseline was re-established.

For reinstatement test, heroin was replaced with saline and cues were removed during extinction training. After reaching extinction (≤ 20 active presses for 2–3 days), rats received MRI-2594 (0, 10, or 30 mg/kg, i.p.) 30 min before and heroin (1 mg/kg, i.p.) 15 min before a reinstatement

session. The complete heroin self-administration and reinstatement procedures are described in the SI.

We also observed the effects of intranasal administration or intracranial microinjections of MRI-2594 into the VTA or NAc on heroin self-administration in rats. The detailed procedures are described in the SI.

Experiment 2: Heroin self-administration in wildtype and CB2-KO-eGFP mice

WT and CB2-KO-eGFP mice were trained for heroin self-administration using a similar protocol as in rats, but with 15 μ l/infusion [26] and mouse operant chambers (Model ENV-307A). Mice received MRI-2594 (0, 10, 30 mg/kg, i.p.) during FR2 sessions in a counterbalanced, within-subject design, with 3–5 days between tests.

Experiment 3: Hot-plate analgesic test in mice

For MRI-2594 analgesic effects, WT and CB2-KO-eGFP mice received MRI-2594 (0, 3, 10, 30 mg/kg, i.p.) and were tested on a 52 °C hot plate (cutoff: 60 s) at 30, 60, 90, and 120 min post-injection. Baseline latencies were recorded pre-treatment. Tests followed a counterbalanced, within-subject design with ≥ 48 h between tests.

To assess interaction with oxycodone analgesia, MRI-2594 (0, 10, or 30 mg/kg, i.p.) was administered 15 min before oxycodone (3 or 10 mg/kg, i.p.). Latencies were measured using the same procedures. The complete procedures are described in the SI.

Experiment 4: Open-field locomotion in WT mice

To test whether MRI-2594 produces sedative effects, we observed the effects of MRI-2594 on open-field locomotion. The complete procedures are described in the SI.

Experiment 5: Fiber photometry for DA measurement

Fiber photometry recordings were conducted in freely moving mice that received intra-NAc microinjections of pAAV-hSyn-GRAB_{DA3m}-cEGFP. The fluorescence signal change ($\Delta F/F_0$) was calculated by subtracting the pre-injection baseline signal (F_0 , defined as the mean value over a 60 s baseline period) and then normalized to F_0 for further analysis. To quantify the DA response to MRI-2594, the area under the curve (AUC) of the $\Delta F/F_0$ signal was calculated using trapezoidal numerical integration over a fixed time window. Detailed fiber photometry analysis methods are provided in the SI.

Experiment 6: Optogenetic intracranial self-stimulation (oICSS) in DAT-Cre mice

DAT-Cre mice received unilateral VTA injections of AAV5-DIO-ChR2-EYFP and optical fibers implants 0.5 mm above the target site. After 4 weeks recovery, mice were trained for oICSS. Stable behavior was followed by a rate-frequency protocol (1 - 100 Hz, 10-min blocks).

MRI-2594 (0, 10, 30 mg/kg) or CB2R antagonist MRI-2687 (0, 10, 30 mg/kg) was injected i.p. 15 min before testing. Mice were returned to baseline between tests. Postmortem immunohistochemistry confirmed ChR2 expression in VTA DA neurons. The complete oICSS procedures are described in the SI.

Experiment 7: GFP-Immunohistochemistry in CB2-KO-eGFP reporter mice

Mice were perfused with saline and 4% PFA. Brains were post-fixed, sectioned (40 μ m), and incubated with rabbit anti-GFP and sheep anti-TH antibodies, followed by Alexa Fluor 555 and 488-conjugated secondaries. Slides were mounted with DAPI medium and imaged via Zeiss LSM510 confocal microscope. Co-localized cells (GFP⁺/TH⁺/DAPI⁺) were counted in ImageJ across 6 slices per brain from 3 animals (see the SI).

DATA ANALYSIS

Data are presented as mean \pm SEM. One-way ANOVAs were used to assess MRI-2594 dose effects on heroin self-administration and reinstatement of drug-seeking behavior. Two-way RM ANOVAs analyzed open-field locomotion, hot-plate analgesia, and oICSS data. Post hoc comparisons were made using Holm-Sidak tests, with significance set at $p < 0.05$.

RESULTS

MRI-2594 reduces heroin-taking and -seeking in rats

To assess MRI-2594's potential in treating OUD, we first examined its effects on heroin self-administration (SA) in rats (Fig. 1A). Systemic MRI-2594 (3, 10, 30 mg/kg, i.p., 30 min prior) significantly reduced heroin infusions (Fig. 1B, C) and active lever presses at high doses (Fig. 1D), without affecting inactive lever presses (Fig. 1E). One-way ANOVA revealed significant treatment main effects (infusions: $F_{3,27} = 4.38$, $p = 0.012$; active presses: $F_{3,27} = 5.97$, $p = 0.003$), with post hoc tests showing reductions at 30 mg/kg for infusions ($p < 0.05$) and at 10 and 30 mg/kg for active presses ($p < 0.01$). Inactive presses were unchanged (Fig. 1E, $F_{3,27} = 0.75$, $p = 0.54$).

MRI-2594 also significantly attenuated heroin-primed reinstatement of drug-seeking behavior at high doses (Fig. 1F). One-way ANOVA confirmed a significant treatment effect (Fig. 1G, $F_{2,24} = 6.84$, $p = 0.004$), with post hoc comparisons revealing reduced active lever responding at 10 and 30 mg/kg ($p < 0.01$). Inactive responses during reinstatement were unaffected (Supplementary Fig. 2).

MRI-2594 has no effect on oral sucrose self-administration in mice

To determine whether MRI-2594 selectively alters heroin self-administration, we observed the effects of MRI-2594 on oral sucrose self-administration in mice. The data showed that MRI-2594, at 10 mg/kg and 30 mg/kg that inhibit heroin self-administration in rats, had no effect on sucrose self-administration (Supplementary Fig. 3). One-way RM ANOVA did not reveal significant treatment main effects on either the number of sucrose deliveries ($F_{2,18} = 0.827$, $p > 0.05$), active lever responses ($F_{2,18} = 1.05$, $p > 0.05$), or inactive lever responses ($F_{2,18} = 1.99$, $p > 0.05$).

MRI-2594 does not impair locomotion

To rule out nonspecific effects on locomotor activity, we observed the effects of the same doses of MRI-2594 on open field locomotion in male and female mice. The results showed that MRI-2594 had no significant effect on locomotion in both sexes (Supplementary Fig. 4A, B). Two-way RM ANOVA showed no main effect of treatment (males: $F_{2,238} = 0.087$, $p = 0.99$; females: $F_{2,238} = 3.36$, $p = 0.064$), but revealed significant effects of time and treatment \times time interaction. Post hoc analysis showed no group differences in males and a transient increase only at 10 min in females ($p < 0.01$).

MRI-2594 also had no effect on oxycodone-induced hyperactivity (2 mg/kg, i.p.) (Supplementary Fig. 4C), suggesting its inhibitory effects on heroin-related behaviors are not due to sedation or motor impairment.

MRI-2594 does not compromise oxycodone analgesia

To determine whether CB2R activation by MRI-2594 affects opioid analgesia – a critical consideration in OUD therapy – we assessed its impact on oxycodone-induced analgesia using the hot-plate test. Given known sex differences in opioid analgesia [48, 49], male and female WT mice were tested with two doses of MRI-2594 (10, 30 mg/kg) combined with two doses of oxycodone (3, 10 mg/kg). MRI-2594, at behaviorally effective doses, did not alter oxycodone-induced analgesia in either sex (Fig. 2A–D). Two-way RM ANOVAs revealed significant time effects (Fig. 2A: $F_{4,56} = 3.31$, $p = 0.024$; Fig. 2B: $F_{4,48} = 11.92$, $p < 0.001$; Fig. 2C: $F_{4,56} = 11.78$, $p < 0.001$; Fig. 2D: $F_{4,48} = 58.24$, $p < 0.001$), but no significant main effects of MRI-2594 treatment (all $p > 0.05$) or treatment \times time interactions (all $p > 0.05$). These findings indicate that MRI-2594 does not compromise opioid analgesia, supporting the therapeutic potential of CB2R agonists for OUD without interfering with pain management.

MRI-2594 alone produces analgesic effects at high doses

We also evaluated the effects of MRI-2594 alone on hot-plate analgesia. There was no difference in basal levels of nociceptive responses to heat stimulation between WT and CB2-KO-eGFP mice following vehicle injection (Fig. 2E). Systemic administration of MRI-2594 (3, 30, and 100 mg/kg) produced mild but significant analgesic effects in WT mice, which were attenuated in CB2-KO-eGFP mice lacking CB2R (Fig. 2F–H). Two-way RM ANOVA revealed a significant main effect of MRI-2594 treatment (Fig. 2F: $F_{4,56} = 5.61$, $p < 0.001$; Fig. 2H: $F_{4,56} = 6.72$, $p < 0.001$), a significant main effect of genotype (Fig. 2F: $F_{1,14} = 6.02$, $p = 0.028$; Fig. 2G: $F_{1,14} = 9.54$, $p = 0.008$; Fig. 2H: $F_{1,14} = 8.08$, $p = 0.013$), and a significant treatment \times time interaction (Fig. 2F: $F_{4,56} = 3.92$, $p = 0.007$; Fig. 2G: $F_{4,56} = 3.51$, $p = 0.013$; Fig. 2H: $F_{4,56} = 3.26$, $p = 0.018$). However, there was no significant main effect of treatment following the 30 mg/kg dose (Fig. 2G: $F_{4,56} = 0.38$, $p = 0.82$). Post hoc comparisons showed significant differences between WT and CB2-KO-eGFP mice, and a significant increase in latency to pain response at 30, 60, 90, and 120 min after administration of various MRI-2594 doses compared to the vehicle control group (Fig. 2F–H).

Intra-VTA or intra-NAC microinjections of MRI-2594 inhibit heroin self-administration in rats

Previous studies have shown that CB2Rs are expressed in the mesolimbic DA system and modulate cocaine-taking and -seeking behavior [26, 50]. To determine whether mesolimbic CB2R activation contributes to MRI-2594's effects on heroin self-administration, we examined the impact of intranasal or intracranial microinjections of MRI-2594 in rats.

We first assessed intranasal delivery, which enables direct drug access to the brain [51], on heroin self-administration. Intranasal administration of MRI-2594 showed a trend toward reducing heroin self-administration as assessed by the number of heroin infusions (Supplementary Fig. 5A, $F_{2,18} = 1.404$, $p = 0.271$) and active lever responses (Supplementary Fig. 5B, $F_{2,18} = 3.072$, $p = 0.071$).

We next examined the effects of direct intra-VTA or intra-NAC administration of MRI-2594 on heroin self-administration. Intra-VTA microinjections significantly reduced the number of heroin infusions (Fig. 3A, $F_{2,16} = 3.739$, $p = 0.047$). Similarly, intra-NAC microinjections of MRI-2594 significantly decreased heroin infusions (Fig. 3B, $F_{2,18} = 3.752$, $p = 0.043$). Post hoc analyses confirmed that administration of 20 μ g MRI-2594 into either the VTA or NAC significantly reduced heroin intake compared to vehicle controls ($p < 0.05$; Fig. 3A, B). Histological examination following the experiments confirmed correct placement of all guide cannula tips in the targeted regions (VTA or NAC) (Supplementary Fig. 6A, C). The corresponding predicted microinjection sites are illustrated in Supplementary Fig. 6(B, D). These findings suggest that CB2R activation within the VTA and NAC contributes to the anti-addictive effects of MRI-2594 observed in this study.

MRI-2594 inhibits dopamine release in the NAC

To assess whether MRI-2594 suppresses dopamine (DA) release, we employed fiber photometry to measure drug-induced changes in DA levels in the NAC (Fig. 3C, D). MRI-2594, at doses of 3, 10, and 30 mg/kg, significantly reduced DA release (Fig. 3F–H, J, K), whereas cocaine (10 mg/kg) produced a robust increase in NAC DA (Fig. 3I, K). One-way RM ANOVA revealed a significant main effect of MRI-2594 treatment (Fig. 3K, $F_{3,21} = 8.93$, $p < 0.001$). Post hoc comparisons showed significant reductions in DA release in the MRI-2594-treated groups compared to vehicle.

MRI-2594 inhibits optical intracranial self-stimulation in DAT-Cre mice

We next investigated the effects of MRI-2594 on dopamine-dependent oICSS behavior maintained by optogenetic stimulation

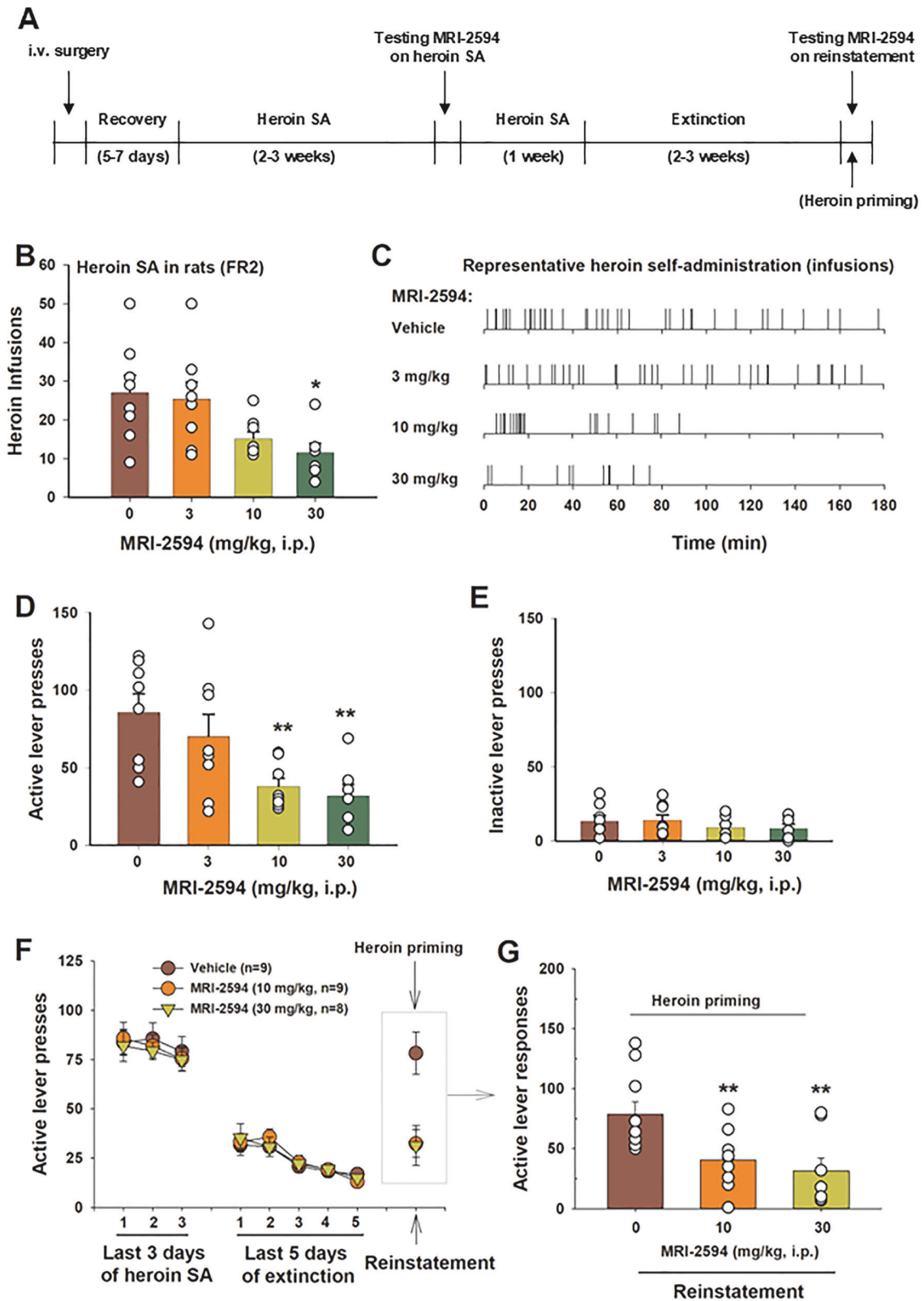


Fig. 1 Effects of MRI-2594 on heroin self-administration and reinstatement of heroin-seeking in rats. **A** Experimental timeline. **(B–E)** MRI-2594 (3, 10 and 30 mg/kg, i.p.) inhibited intravenous heroin self-administration, as assessed by reductions in heroin infusions (**B**), representative self-administration patterns (**C**), and active lever presses (**D**), with no effect on inactive lever presses (**E**). **F** Time course of active lever responses during the last three sessions of heroin self-administration, five extinction sessions, and the reinstatement test. **G** MRI-2594 (10 and 30 mg/kg, i.p.) significantly attenuated heroin (1 mg/kg, i.p.)-primed reinstatement of drug-seeking behavior. * $p < 0.05$, ** $p < 0.01$, compared to vehicle.

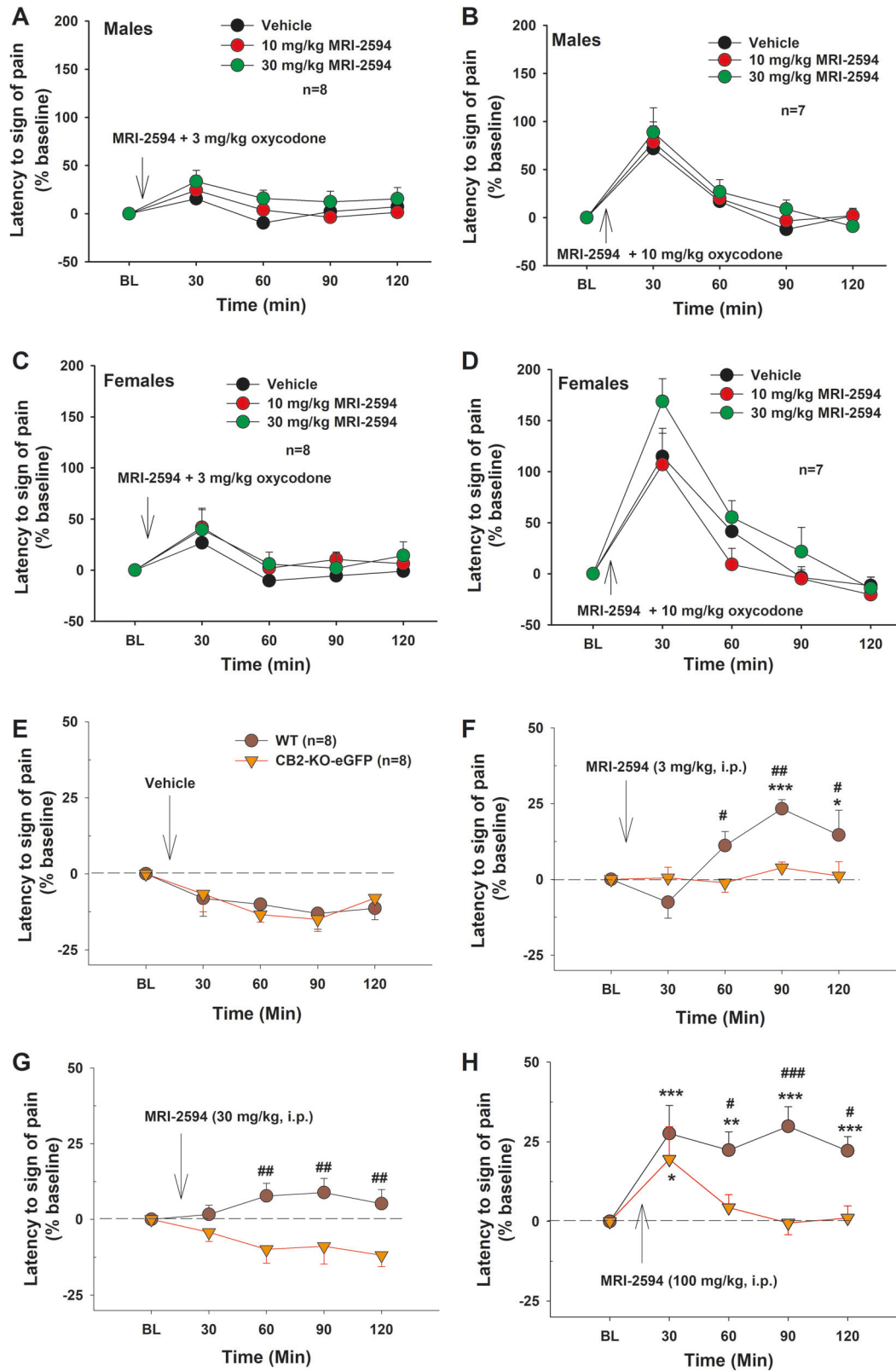
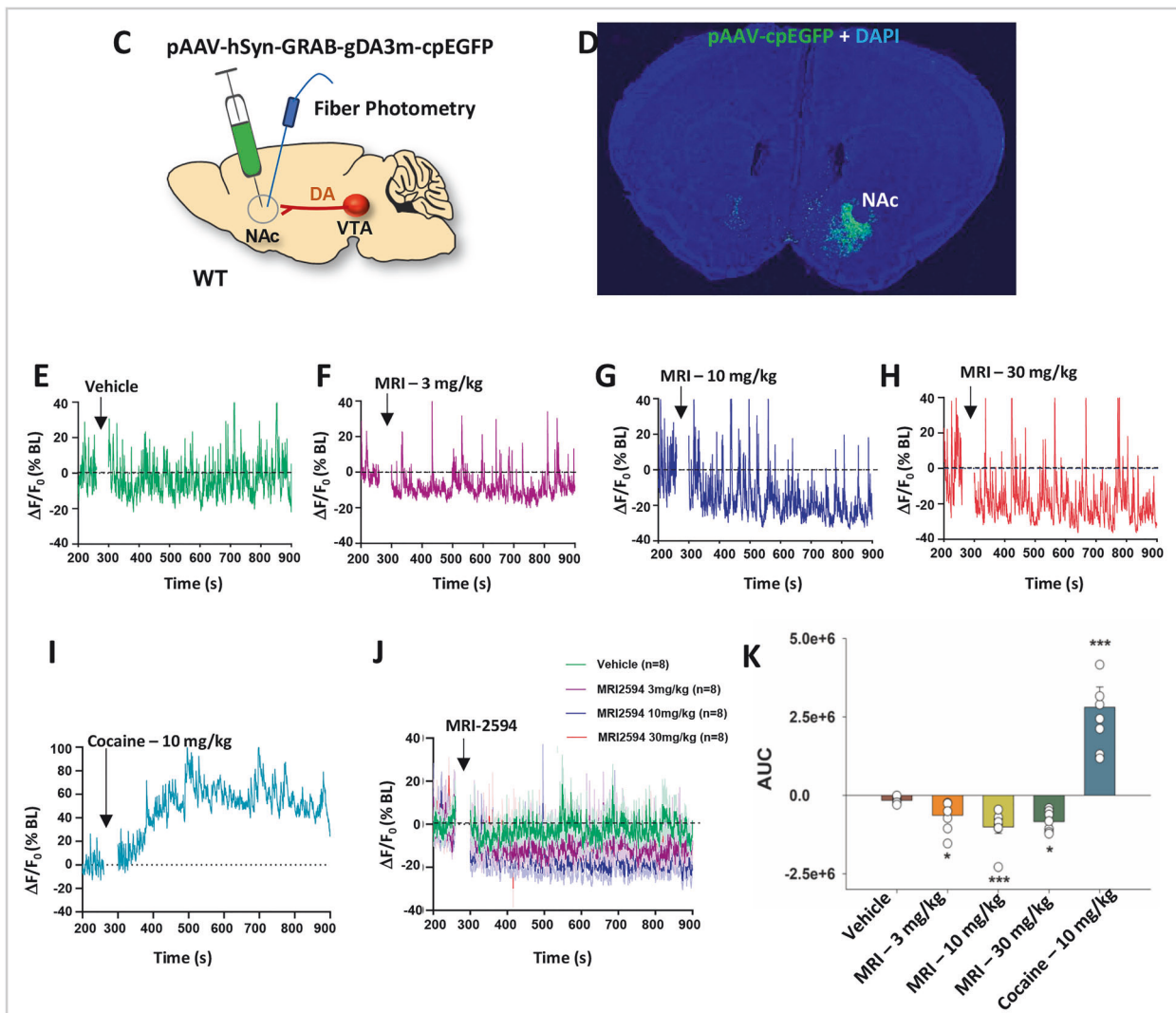
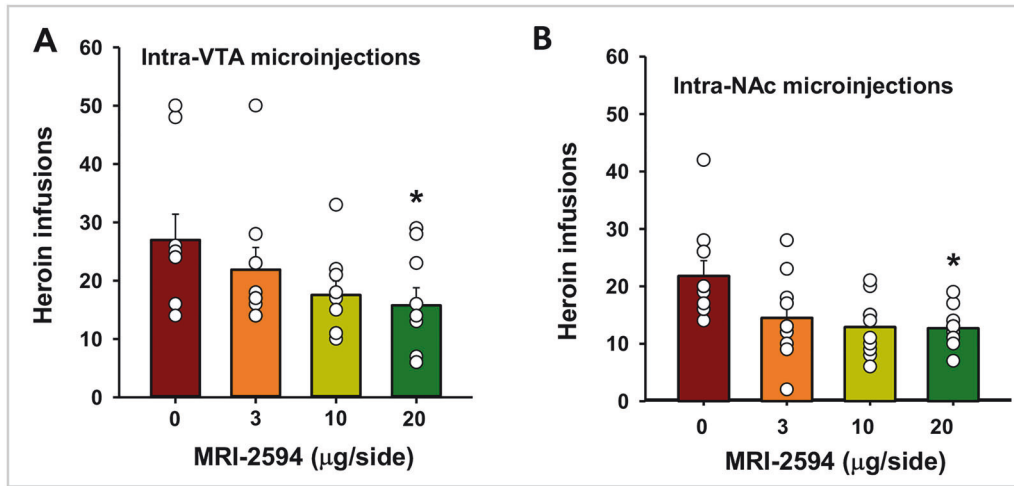


Fig. 2 Effects of MRI-2594 on oxycodone-induced analgesia in male and female mice and the effects of MRI-2594 alone on thermal nociceptive response. (A, B) Systemic administration of MRI-2594 did not significantly alter oxycodone-induced hot-plate analgesia in male mice at either 3 mg/kg (A) or 10 mg/kg (B) of oxycodone. (C, D) Similarly, MRI-2594 had no effect on oxycodone-induced analgesia in female mice at 3 mg/kg (C) or 10 mg/kg (D) of oxycodone. (E–H) MRI-2594 alone (3, 30, or 100 mg/kg) induced dose-dependent analgesia in wild-type (WT), but not CB2-KO-eGFP, mice. * $p < 0.05$, ** $p < 0.01$, *** $p < 0.001$, compared to baseline (BL). # $p < 0.05$, ## $p < 0.01$, ### $p < 0.001$, compared to CB2-KO-eGFP mice.



of VTA DA neurons in DAT-Cre mice (Fig. 4A-C). Systemic administration of MRI-2594 dose-dependently inhibited oICSS, shifting the stimulation-response curve downward. Notably, these inhibitory effects were blocked by co-administration of MRI-2687, a selective CB2R antagonist (Fig. 4E). A two-way RM ANOVA

revealed a significant main effect of MRI-2594 treatment (Fig. 4E, $F_{3,27} = 6.943$, $p = 0.001$), a significant frequency main effect ($F_{5,135} = 62.562$, $p < 0.001$) and a significant treatment \times frequency interaction ($F_{15,135} = 5.076$, $p < 0.001$). Post-hoc analysis showed that 30 mg/kg MRI-2594 significantly inhibited lever responses for

Fig. 3 Effects of intracranial microinjections of MRI-2594 on heroin self-administration in rats and effects of systemic MRI-2594 on DA release in the NAc in WT mice. **A** Intra-VTA administration of MRI-2594 reduced heroin self-administration at high doses. **B** Intra-NAc administration of MRI-2594 also decreased heroin intake. * $p < 0.05$, compared to vehicle. **C** Schematic of fiber photometry setup for DA measurement. WT mice received intra-NAc microinjections of pAAV-hSyn-GRAB_{DA3m}-cpEGFP, followed by implantation of a fiber-optrode to record fluorescent DA signal. **D** Representative image showing EGFP expression in the NAc following unilateral injection of pAAV-hSyn-GRAB_{DA3m}-cpEGFP. **(E–H)** Representative traces of DA signals from a single WT mouse with increasing doses, showing a significant reduction in DA levels at all three doses tested. **I** In contrast, cocaine (10 mg/kg, i.p.) produced a robust increase in DA. **J** Averaged DA signals before and after vehicle or three doses of MRI-2594, illustrating dose-related suppression. **K** Averaged area under the curve (AUC) data following MRI-2594 or cocaine administration. * $p < 0.05$, *** $p < 0.001$, compared to vehicle; $n = 8$ per group.

brain-stimulation reward at 25 Hz ($p = 0.011$), 50 Hz ($p < 0.001$), and 100 Hz ($p < 0.001$) compared to vehicle controls. In contrast, MRI-2687 alone had no effect on oICSS ($F_{2,100} = 0.600$, $p = 0.559$; Fig. 4F). These findings suggest that CB2R activation inhibits DA-dependent behaviors.

CB2-driven GFP expression in midbrain dopamine neurons in CB2-KO-eGFP mice

Several studies have reported functional CB2R expression in midbrain dopamine and glutamate neurons, as well as in other brain regions, using multiple complementary approaches – such as IHC, in situ hybridization, electrophysiology, pharmacology, and behavioral analyses in both WT and CB2-KO mice [22, 26, 40, 42, 50, 52, 53]. In contrast, findings from two transgenic CB2-GFP reporter mouse lines showed GFP signals only in microglia, not in neurons, either in healthy mice [44] or in 5xFAD Alzheimer's disease mice [45]. This discrepancy has raised questions about whether CB2R is truly expressed in the brain and specifically within neurons. By examining the GFP knock-in strategies used in these lines, we found that the GFP or EGFP knock-in approaches may not reflect endogenous CB2R expression as stated in the introduction above (Supplementary Fig. 1).

To address this, we generated a new CB2R reporter mouse line in which the CB2R coding region was replaced with eGFP (Fig. 5A), ensuring that GFP expression was fully driven by the endogenous CB2R regulatory elements during transcription and translation. This resulted in a dual CB2-KO and CB2-GFP reporter line (CB2-KO-eGFP) (Supplementary Fig. 1).

Using IHC assays with a GFP antibody, we detected robust GFP expression in both tyrosine hydroxylase (TH)-positive DA neurons within the VTA of CB2-KO-eGFP mice, but not in WT controls, as shown by GFP and TH co-localization (Fig. 5B–D; Supplementary Fig. 7). GFP was also detected in a subset of TH-negative non-DA neurons (Supplementary Fig. 8). These findings in this new strain of CB2-KO-eGFP mice are fully consistent with our previous findings with CB2R IHC and RNAscope ISH assays [50, 54].

We also examined GFP expression in the striatum. While GFP signal was relatively weak in the NAc (Supplementary Fig. 9) compared to the dorsal striatum (Supplementary Fig. 10) or the VTA (Fig. 5; Supplementary Fig. 7), we observed GFP expression in some DAPI-labeled cells, suggesting potential CB2R expression in postsynaptic neurons within the striatum.

MRI-2594 inhibits heroin self-administration in WT but not in CB2-KO-eGFP mice

Lastly, we used the CB2-KO-eGFP mice as negative controls to determine whether the reduction in heroin self-administration induced by MRI-2594 is mediated via CB2R activation. We first compared heroin self-administration behavior between WT littermates and CB2-KO-eGFP mice, in both males and females. There were no significant differences in the acquisition and maintenance of heroin self-administration between the two genotypes in either sex, as assessed by heroin infusions (Fig. 6A, B), and active and inactive lever presses (Supplementary Fig. 11). Therefore, data from male and female mice were combined for further analysis.

Systemic administration of MRI-2594 significantly reduced heroin infusions and active lever presses under a FR2 schedule in WT mice (Fig. 6C, E), but not in CB2-KO-eGFP mice (Fig. 6D, F). A one-way RM ANOVA revealed a significant main effect of MRI-2594 treatment on heroin infusions (Fig. 6C, $F_{2,18} = 5.551$, $p = 0.013$) and active lever responses (Fig. 6E, $F_{2,18} = 3.979$, $p = 0.037$) in WT mice. In contrast, no significant treatment effects were observed in CB2-KO-eGFP mice (Fig. 6D, $F_{2,16} = 0.904$, $p = 0.086$; Fig. 6F, $F_{2,16} = 2.529$, $p = 0.111$).

Additionally, one-way RM ANOVA revealed no significant treatment effects on inactive lever responses in either WT (Fig. 6E, $F_{2,18} = 0.248$, $p = 0.783$) or CB2-KO-eGFP mice (Fig. 6F, $F_{2,16} = 1.447$, $p = 0.264$), indicating the specificity of MRI-2594's effects on heroin-directed behavior. These findings support the conclusion that MRI-2594 reduces heroin self-administration through a CB2R mechanism.

DISCUSSION

In this study, we systematically evaluated the therapeutic potential of MRI-2594, a novel and highly selective CB2 receptor (CB2R) agonist, for treating opioid use disorder (OUD). Our findings demonstrate that systemic administration of MRI-2594 significantly reduced heroin self-administration under an FR2 reinforcement schedule and inhibited heroin-primed reinstatement of drug-seeking behavior in rats, indicating its potential utility in treating OUD. Importantly, MRI-2594 did not alter oral sucrose self-administration, open-field locomotion, and opioid analgesia, while itself produced mild but significant analgesia. This pharmacological profile suggests that MRI-2594 may have therapeutic potential for OUD without compromising therapeutic pain relief.

Furthermore, systemic administration of MRI-2594 inhibited DA release in the NAc, and direct infusion of MRI-2594 into either the VTA or NAc also significantly suppressed heroin self-administration. Optogenetic activation of VTA DA neurons produced robust optical brain-stimulation reward, which was likewise inhibited by MRI-2594. This effect was blocked by pretreatment with MRI-2687, a selective CB2R antagonist, indicating that the CB2R mechanisms in the mesolimbic DA system at least in part contribute to the anti-addictive effects of MRI-2594. Consistent with these findings, in a novel strain of CB2-KO-eGFP mice, endogenous CB2R-driven GFP expression was observed in midbrain DA neurons, and genetic deletion of CB2Rs abolished MRI-2594's behavioral effects. Together, these results support a CB2R-dependent mechanism through which MRI-2594 inhibits opioid-taking and -seeking behaviors, identifying brain CB2Rs as a potential therapeutic target for OUD.

CB2R agonists as promising treatments for substance use disorders

Preclinical research has provided compelling evidence that CB2Rs play a critical role in modulating addiction-related behaviors, particularly in models of cocaine and alcohol use disorders [11, 22, 55, 56]. CB2R agonists consistently reduce cocaine-induced hyperlocomotion, self-administration, conditioned place

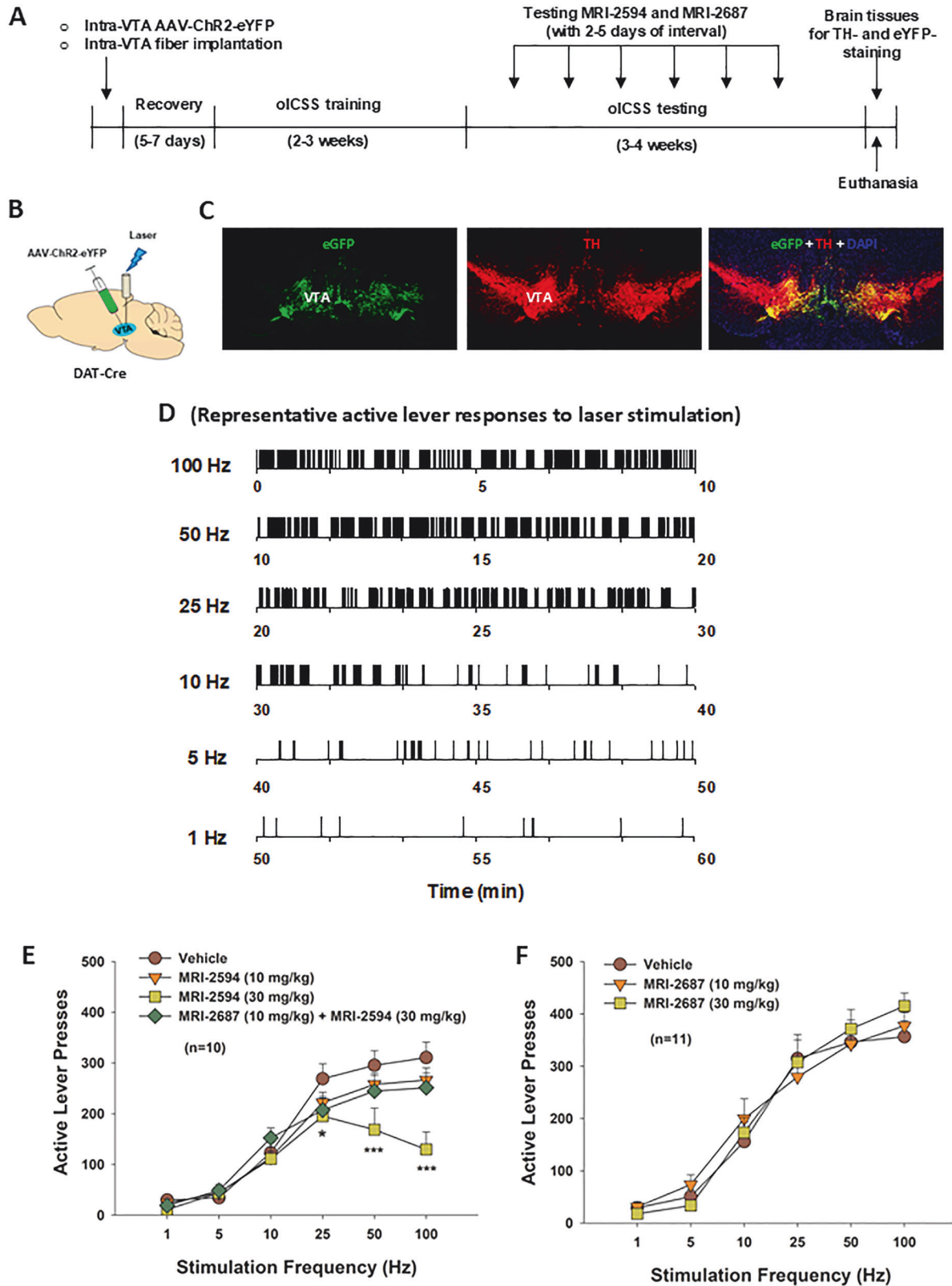


Fig. 4 Effects of MRI-2594 on optical intracranial self-stimulation (oICSS) in DAT-Cre mice. A Experimental timeline for oICSS. **B** Schematic of oICSS setup. DAT-Cre mice received intra-VTA microinjections of AAV-DIO-ChR2-eYFP, followed by implantation of a fiber-optrode to enable optogenetic stimulation of VTA DA neurons contingent on lever pressing. **C** Representative images showing TH immunostaining (red) and ChR2-eYFP expression (green) in the VTA, confirming co-localization in DA neurons. **D** Representative oICSS behavior from a single mouse across descending stimulation frequencies (10 min per frequency), demonstrating frequency-dependent self-stimulation. **E** Systemic administration of MRI-2594 dose-dependently shifted the stimulation–response curve downward, indicating a reduction in brain-stimulation reward. This effect was blocked by MRI-2687, a selective CB2R antagonist. **F** Systemic administration of MRI-2687 alone had no effect on oICSS behavior. *** $p < 0.001$, compared to vehicle.

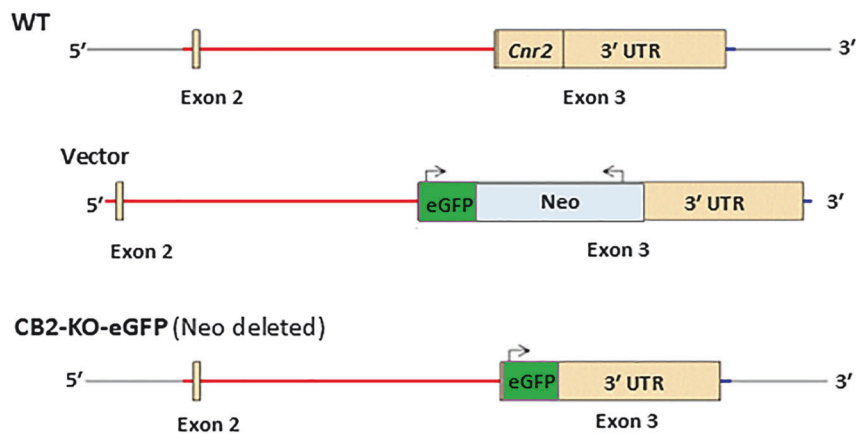
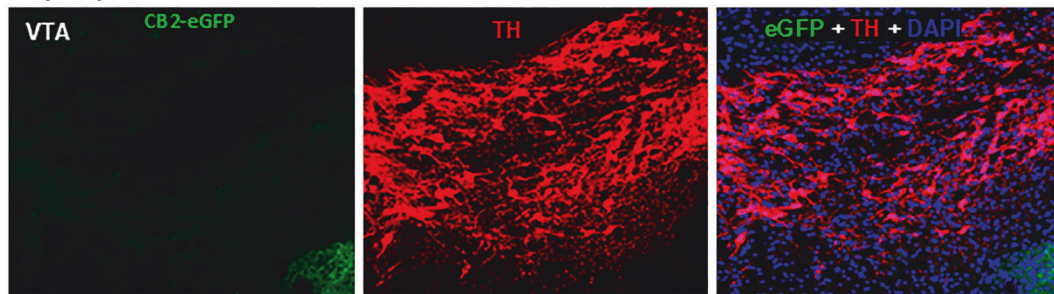
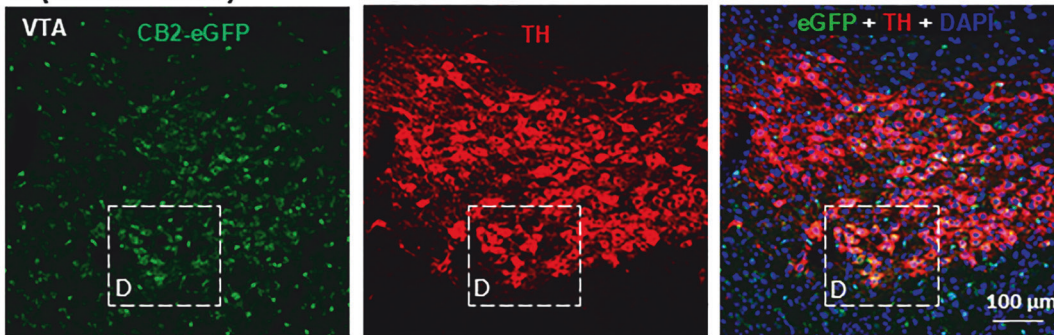
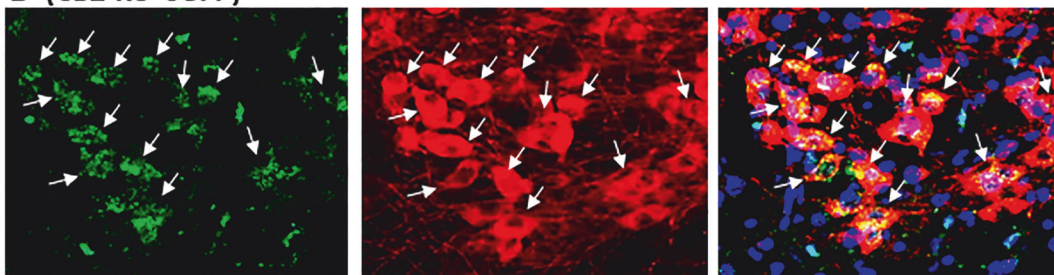
A (CB2R gene structures)**B (WT)****C (CB2-KO-eGFP)****D (CB2-KO-eGFP)**

Fig. 5 CB2R-driven GFP expression in CB2-KO-eGFP mice. **A** Schematic of CB2 gene targeting. Upper panel: Wild-type (WT) CB2 gene structure with yellow boxes indicating exons 2 and 3; exon 3 contains the CB2 coding region (*Cnr2*). Middle panel: CB2-eGFP-Neo-FRT targeting construct, in which the entire CB2 gene is replaced by an eGFP-Neo cassette. Lower panel: Final gene structure in CB2-KO-eGFP mice following Neo deletion via Flp recombinase. **B** GFP immunostaining using a primary anti-GFP antibody (Invitrogen) and a fluorescent secondary antibody (Alexa Fluor 555). No GFP signal was detected in the VTA of WT mice. **C** In CB2-KO-eGFP mice, GFP signal was observed in VTA TH-positive (DA) neurons. **D** Magnified images of boxed regions in panel C, showing colocalization of GFP and TH in VTA DA neurons. (see Suppl. Figures 7 and 8).

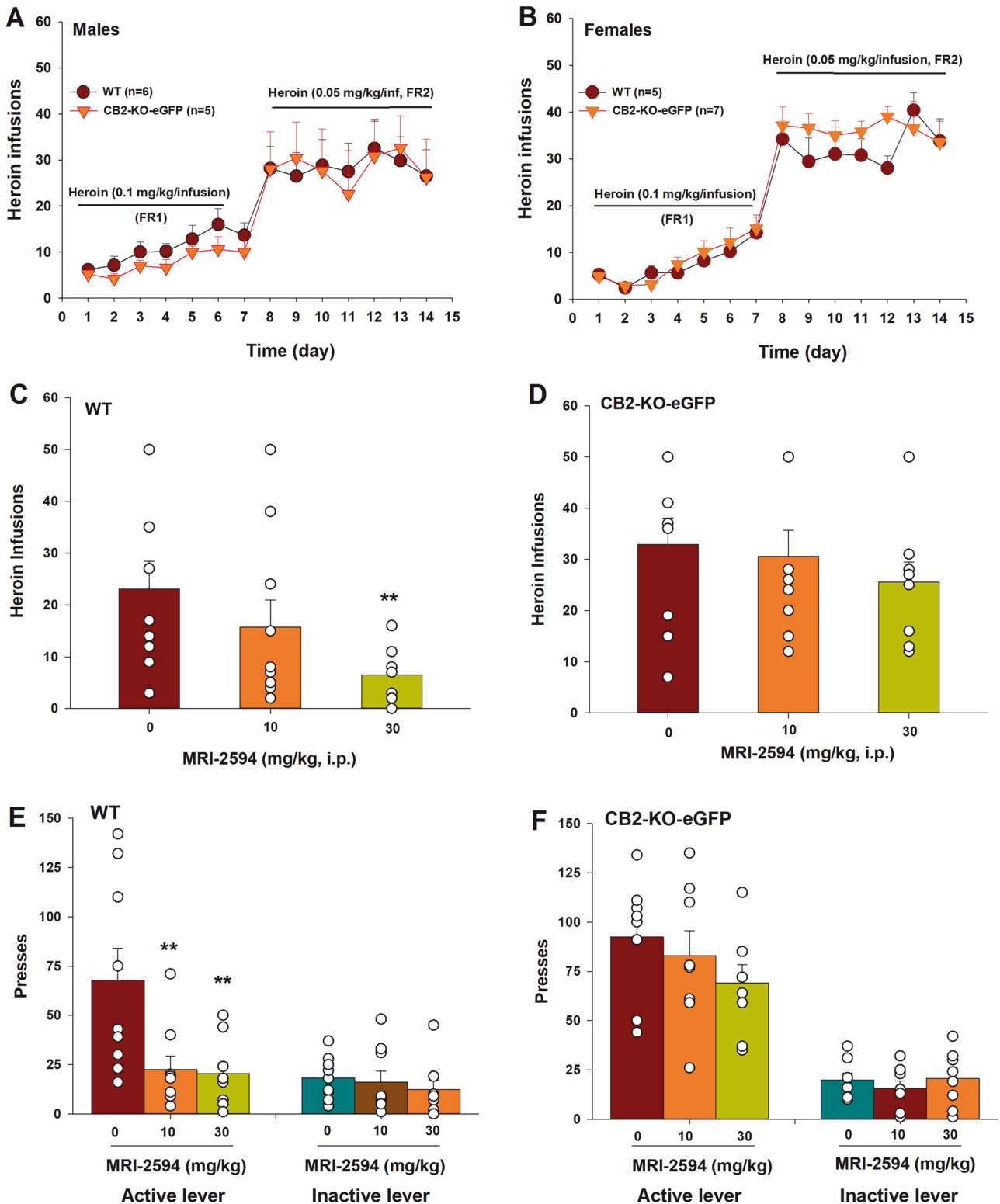


Fig. 6 Effects of MRI-2594 on heroin self-administration under FR2 reinforcement in WT and CB2-KO-eGFP mice. (A, B) Acquisition and maintenance of heroin self-administration at various doses under FR1 and FR2 schedules in male (A) and female (B) mice. No significant genotype differences were observed. (C, D) MRI-2594 (10, 30 mg/kg, i.p.) significantly reduced heroin infusions in WT (C) but not CB2-KO-eGFP (D) mice. (E, F) MRI-2594 reduced active lever presses in WT (E) but not CB2-KO-eGFP (F) mice. ** $p < 0.01$, compared to vehicle.

preference (CPP), and striatal dopamine release in rats and WT mice, but not in CB2-KO mice [26, 50, 54, 57]. Similarly, CB2R activation reduces voluntary alcohol intake, preference, and anxiety-like behavior associated with chronic alcohol exposure [58, 59]. CB2R

agonists also attenuate nicotine self-administration and nicotine-seeking behaviors in both rats and mice – effects blocked by CB2R antagonism [29]. Conversely, CB2R antagonism has been shown to increase alcohol consumption [58].

Mice overexpressing CB2Rs exhibit reduced cocaine self-administration, cocaine-induced CPP, and locomotor sensitization and can even shift cocaine CPP to aversion [28], whereas CB2R deletion in dopaminergic neurons enhances locomotion and cocaine CPP [60]. CB2-KO mice also show increased alcohol preference and intake [61], suggesting a protective role for CB2R activation. Similarly, cannabidiol (CBD) reduces voluntary alcohol intake and protects against alcohol-induced neurodegeneration [62], suggesting that cannabinoid-based therapies broadly mitigate drug-induced neural adaptations. Unlike Δ^9 -THC and CBD, which act as both CB1 and CB2 receptors and additional targets [63], MRI-2594 is a highly potent and selective CB2R agonist with minimal off-target activity [38, 39]. This specificity may improve its therapeutic potential for SUDs while minimizing adverse psychoactive effects. Although CB2R is implicated in cocaine and alcohol addiction, the role of CB2R in OUD remains relatively unexplored.

Our study addresses this gap, demonstrating that MRI-2594 significantly reduces heroin self-administration and heroin-primed reinstatement in both rats and mice, complementing prior findings that CB2R agonists such as LY2828360 attenuated morphine-induced CPP in rats and WT mice but not in CB2-KO mice [36, 64], and that β -caryophyllene reduced heroin self-administration in rats and heroin-induced CPP in mice [65]. We note that MRI-2594 shows very high binding affinity and potency at hCB2R *in vitro* [38, 39]. However, the much higher doses (10, 30 mg/kg, *i.p.*) are required *in vivo* to inhibit drug-taking and drug-seeking behaviors, which may be related to its limited blood–brain barrier penetration and rapid metabolism.

Notably, MRI-2594 pretreatment produced a trend toward an increase in oxycodone-induced analgesia, while itself produced mild analgesic effects. This is consistent with previous findings that CB2R activation by AM1710 or LY2828360 reduces morphine tolerance and physical dependence [37, 38, 66], where deletion of CB2R exacerbated morphine withdrawal in CB2-KO mice [64]. These observations underscore the unique pharmacological potential of CB2R agonists to reduce opioid reward, relapse, and dependence while preserving or even enhancing analgesic efficacy.

Although these positive findings, possible translational limitations must be considered as CB2R exhibits species differences in gene splicing, transcript variants, amino acid sequences, brain distribution, and ligand sensitivity [67, 68]. This highlights the need for caution when extrapolating preclinical findings to human OUD. Future studies in non-human primates and humanized models will be essential to further assess its translational potential.

Neural mechanisms underlie MRI-2594 action

Another key finding of this study is the involvement of dopaminergic mechanisms in mediating MRI-2594's anti-addiction effects. CB2Rs have historically been viewed as peripheral receptors, and their expression in the brain has been debated [69]. To distinguish between peripheral and central effects, we tested intranasal delivery of MRI-2594, which enables direct drug access to the brain [51]. Although intranasal administration showed a trend toward reducing heroin self-administration, its efficacy was limited, likely due to technical issues such as sneezing and drug leakage in lightly anesthetized rats.

In contrast, direct administration of MRI-2594 into the VTA or NAc produced dose-dependent reductions in heroin self-administration in rats, reinforcing the role of brain CB2Rs in mediating its effects. These findings are consistent with previous work showing that JWH133, another CB2R agonist, dose-dependently inhibited cocaine self-administration when delivered intranasally or into the NAc [26].

To further confirm a dopaminergic mechanism, we used fiber photometry to measure NAc DA response to MRI-2594. The data

showed that MRI-2594 inhibited DA release in the NAc. Furthermore, optogenetic stimulation of VTA DA neurons produced robust *o*ICSS response, which was also reduced by MRI-2594. Notably, this inhibitory effect was blocked by MRI-2687, a CB2R antagonist, suggesting that MRI-2594 reduces DA-mediated reward through CB2R activation. Supporting this, β -caryophyllene also attenuated *o*ICSS and heroin-enhanced *o*ICSS in DAT-Cre mice (29, 65). While these findings highlight a dopaminergic mechanism, it is important to note that CB2Rs are also expressed in non-DA neurons [41, 70], which may contribute directly or indirectly to the effects of CB2R agonists. This non-dopaminergic mechanism may also help explain why MRI-2594, at 30 mg/kg, did not produce a greater reduction in NAc DA release compared to lower doses (3 and 10 mg/kg) as its non-DA action, such as CB2R activation in GABA neurons, may functionally compromise DA-mediated effects.

In addition, CB2Rs are also expressed in peripheral primary sensory neurons, where they functionally modulate nociception and opioid action [66, 71]. Selective deletion of CB2Rs from dorsal root ganglion (DRG) neurons attenuates the analgesic efficacy of CB2R agonists and abolishes their ability to spare morphine tolerance [36, 66]. Moreover, coadministration of a sub-effective dose of the CB2R agonist AM1241 with morphine reduces tolerance development, accompanied by increased MOR expression in the DRG and spinal cord [72]. These findings suggest that peripheral CB2R mechanisms may also contribute to the analgesic and anti-addictive effects of MRI-2594 observed in this study.

Identification of CB2-driven GFP expression in midbrain DA neurons

Another major contribution of this study is the identification of endogenous CB2R expression in the brain and midbrain DA neurons using a novel CB2-KO-eGFP reporter mouse line. The presence of CB2Rs in the brain – especially in neurons – has long been controversial [22, 40, 69]. Early studies failed to detect CB2R mRNA in the brain using classical *in situ* hybridization and northern blot methods [73–75]. However, more sensitive techniques, such as RNAscope *in situ* hybridization, immunolabeling, electrophysiology, and behavioral pharmacology, combined with the use of constitutive and conditional CB2-KO mice, have provided strong evidence supporting neuronal CB2R expression in midbrain DA and glutamate neurons [22, 41, 50, 54], hippocampal glutamate neurons [42, 76], and accumbens GABA neurons [70].

Surprisingly, two prior CB2R reporter lines failed to detect GFP expression in neurons [44] or microglia in the brains of healthy mice [45], raising doubts about CB2R expression in the brain, particularly in neurons. However, analysis of GFP knock-in strategies in these mouse lines revealed significant limitations. In CB2-GFP BAC transgenic mice [44], the GFP gene was randomly integrated into the genome, with an unknown insertion site, copy number, and size. Since the endogenous CB2R gene remains intact, GFP expression may be influenced by epigenetic factors and may not reflect endogenous CB2R expression (Supplementary Fig. 1A). If the BAC construct integrates into the mouse CB2 gene, it may disrupt endogenous CB2R expression, but the endogenous CB2 promoter would unlikely regulate BAC-driven CB2R expression. In the CB2^{EGFP/f/f} mouse line [45], a dual-gene knock-in strategy was employed – two loxP sites were inserted on both sides of the CB2 gene, and an IRES-EGFP cassette was introduced into the 3' untranslated region (UTR) via homologous recombination. This generated a dual CB2-flox and EGFP reporter mouse line. While this design enables the Cre-LoxP techniques used to generate conditional CB2-KO mice, it raises concerns regarding its reliability as a CB2-GFP reporter model. First, the insertions of two loxP sites and the IRES-EGFP cassette into the 5' and 3' UTRs may interfere with endogenous CB2R transcription and translation (Supplementary Fig. 1B). Second, because the IRES-EGFP is

positioned in the 3' UTR downstream of the CB2R translation stop codon, GFP expression is unlikely to be driven by the native CB2R translation machinery (Supplementary Fig. 1B). Third, while endogenous CB2R translation is 5' cap-dependent [77], IRES-driven EGFP expression is cap-independent and bypasses the native 5' UTR structure. As a result, GFP expression in CB2^{EGFP/f/f} mice may also not reflect endogenous CB2R expression.

To overcome these issues, we developed a novel strain of CB2-KO-eGFP reporter mice in which the entire CB2R coding region was replaced with eGFP, while preserving native 5' and 3' UTRs (Supplementary Fig. 1C). This ensures that GFP expression is driven by the endogenous CB2R promoter and translation machinery, enabling reliable reporting of CB2R expression. Using this model, we observed GFP signals in VTA DA neuron, but not in WT controls, supporting midbrain CB2R expression. We also observed GFP expression in striatal cells, though the specific cell types remain to be identified. Behaviorally, MRI-2594 reduced heroin self-administration in WT but not in CB2-KO-eGFP mice, confirming the role of CB2Rs in mediating its anti-addictive effects.

In conclusion, our findings demonstrate that the selective CB2R agonist MRI-2594 inhibits heroin self-administration and heroin-triggered reinstatement of drug-seeking behavior in rats and WT mice, but not in CB2-KO-eGFP mice. MRI-2594 also inhibits NAc DA release and DA-dependent brain-stimulation reward and induces mild analgesia without impairing opioid analgesic effects. The presence of CB2-driven GFP expression in midbrain DA neurons also supports a dopaminergic CB2R mechanism. These findings establish brain CB2Rs as a potential therapeutic target for OUD and highlight MRI-2594 as a promising candidate for further development.

DATA AVAILABILITY

All the raw data in this paper is available upon request.

REFERENCES

- Rudd RA, Aleshire N, Zibbell JE, Gladden RM. Increases in drug and opioid overdose deaths—United States, 2000–2014. *MMWR Morb Mortal Wkly Rep*. 2016;64:1378–82.
- Ahmad FB, Cisewski JA, Rossen LM, Sutton P. Provisional drug overdose death counts. National Center for Health Statistics. *Center for Disease Control and Prevention* 2023.
- Hedegaard H, Bastian BA, Trinidad JP, Spencer M, Warner M. Drugs most frequently involved in drug overdose deaths: United States, 2011–2016. *Natl Vital Stat Rep*. 2018;67:1–14.
- Kenan K, Mack K, Paulozzi L. Trends in prescriptions for oxycodone and other commonly used opioids in the United States, 2000–2010. *Open Med*. 2012;6:e41–47.
- Novick DM, Saltsitz EA, Joseph H, Kreek MJ. Methadone medical maintenance: an early 21st-century perspective. *J Addict Dis*. 2015;34:226–37.
- Cerda M, Santaella J, Marshall BD, Kim JH, Martins SS. Nonmedical prescription opioid use in childhood and early adolescence predicts transitions to heroin use in young adulthood: a national study. *J Pediatr*. 2015;167:605–612.e601–602.
- Megens AA, Artois K, Vermeire J, Meert T, Awouters FH. Comparison of the analgesic and intestinal effects of fentanyl and morphine in rats. *J Pain Symptom Manage*. 1998;15:253–7.
- Wang XF, Galaj E, Bi GH, Zhang C, He Y, Zhan J, et al. Different receptor mechanisms underlying phytocannabinoid- versus synthetic cannabinoid-induced tetrad effects: opposite roles of CB(1)/CB(2) versus GPR55 receptors. *Br J Pharmacol*. 2020;177:1865–80.
- Malan TP Jr, Ibrahim MM, Lai J, Vanderah TW, Makriyannis A, Porreca F. CB2 cannabinoid receptor agonists: pain relief without psychoactive effects? *Curr Opin Pharmacol*. 2003;3:62–67.
- Hashiesh HM, Sharma C, Goyal SN, Jha NK, Ojha S. Pharmacological properties, therapeutic potential and molecular mechanisms of JWH133, a CB2 receptor-selective agonist. *Front Pharmacol*. 2021;12:702675.
- Galaj E, Xi ZX. Potential of cannabinoid receptor ligands as treatment for substance use disorders. *CNS Drugs*. 2019;33:1001–30.
- Soler-Cedeño O, Alton H, Bi GH, Linz E, Ji L, Makriyannis A, et al. AM6527, a neutral CB1 receptor antagonist, suppresses opioid taking and seeking, as well as cocaine seeking in rodents without aversive effects. *Neuropsychopharmacology*. 2024;49:1678–88.
- Soler-Cedeño O, Xi ZX. Neutral CB1 receptor antagonists as pharmacotherapies for substance use disorders: rationale, evidence, and challenge. *Cells*. 2022;11:3262.
- Galaj E, Hempel B, Moore A, Klein B, Bi GH, Gardner EL, et al. Therapeutic potential of PIMSR, a novel CB1 receptor neutral antagonist, for cocaine use disorder: evidence from preclinical research. *Transl Psychiatry*. 2022;12:286.
- Lujan MA, Kim Y, Zhang LY, Cheer JF. Cannabinoid-based pharmacology for the management of substance use disorders. *Curr Top Behav Neurosci*. 2026;76:297–338.
- He XH, Galaj E, Bi GH, He Y, Hempel B, Wang YL, et al. beta-caryophyllene, an FDA-approved food additive, inhibits methamphetamine-taking and methamphetamine-seeking behaviors possibly via CB2 and Non-CB2 receptor mechanisms. *Front Pharmacol*. 2021;12:722476.
- Zhang J, Wang N, Chen B, Wang Y, He J, Cai X, et al. Blockade of Cannabinoid CB1 receptor attenuates the acquisition of morphine-induced conditioned place preference along with a downregulation of ERK, CREB phosphorylation, and BDNF expression in the nucleus accumbens and hippocampus. *Neurosci Lett*. 2016;630:70–76.
- Sam AH, Salem V, Ghatei MA. Rimonabant: from RIO to ban. *J Obes*. 2011;2011:432607.
- Di Marzo V, Despres JP. CB1 antagonists for obesity—what lessons have we learned from rimonabant? *Nat Rev Endocrinol*. 2009;5:633–8.
- Christensen R, Kristensen PK, Bartels EM, Bliddal H, Astrup A. Efficacy and safety of the weight-loss drug rimonabant: a meta-analysis of randomised trials. *Lancet*. 2007;370:1706–13.
- Manzanares J, Cabanero D, Puente N, Garcia-Gutierrez MS, Grandes P, Maldonado R. Role of the endocannabinoid system in drug addiction. *Biochem Pharmacol*. 2018;157:108–21.
- Jordan CJ, Xi ZX. Progress in brain cannabinoid CB(2) receptor research: From genes to behavior. *Neurosci Biobehav Rev*. 2019;98:208–20.
- Gonzalez-Cuevas G, Martin-Fardon R, Kerr TM, Stouffer DG, Parsons LH, Hammell DC, et al. Unique treatment potential of cannabidiol for the prevention of relapse to drug use: preclinical proof of principle. *Neuropsychopharmacology*. 2018;43:2036–45.
- Al Mansouri S, Ojha S, Al Maamari E, Al Ameri M, Nurulain SM, Bahi A. The cannabinoid receptor 2 agonist, beta-caryophyllene, reduced voluntary alcohol intake and attenuated ethanol-induced place preference and sensitivity in mice. *Pharmacol Biochem Behav*. 2014;124:260–8.
- Onaivi ES, Carpio O, Ishiguro H, Schanz N, Uhl GR, Benno R. Behavioral effects of CB2 cannabinoid receptor activation and its influence on food and alcohol consumption. *Ann N Y Acad Sci*. 2008;1139:426–33.
- Xi ZX, Peng XQ, Li X, Song R, Zhang HY, Liu QR, et al. Brain cannabinoid CB(2) receptors modulate cocaine's actions in mice. *Nat Neurosci*. 2011;14:1160–6.
- Delis F, Polissidis A, Poulia N, Justinova Z, Nomikos GG, Goldberg SR, et al. Attenuation of cocaine-induced conditioned place preference and motor activity via cannabinoid CB2 receptor agonism and CB1 receptor antagonism in rats. *Int J Neuropsychopharmacol*. 2017;20:269–78.
- Aracil-Fernandez A, Trigo JM, Garcia-Gutierrez MS, Ortega-Alvaro A, Ternianov A, Navarro D, et al. Decreased cocaine motor sensitization and self-administration in mice overexpressing cannabinoid CB(2) receptors. *Neuropsychopharmacology*. 2012;37:1749–63.
- He Y, Galaj E, Bi GH, Wang XF, Gardner E, Xi ZX. beta-Caryophyllene, a dietary terpenoid, inhibits nicotine taking and nicotine seeking in rodents. *Br J Pharmacol*. 2020;177:2058–72.
- Ignatowska-Jankowska BM, Muldoon PP, Lichtman AH, Damaj MI. The cannabinoid CB2 receptor is necessary for nicotine-conditioned place preference, but not other behavioral effects of nicotine in mice. *Psychopharmacology*. 2013;229:591–601.
- Navarrete F, Rodriguez-Arias M, Martin-Garcia E, Navarro D, Garcia-Gutierrez MS, Aguilar MA, et al. Role of CB2 cannabinoid receptors in the rewarding, reinforcing, and physical effects of nicotine. *Neuropsychopharmacology*. 2013;38:2515–24.
- Zhang XY, Gamaledin I, Zvonok A, Makriyannis A, Goldberg SR, Le Foll B. Effects of a selective cannabinoid CB2 agonist and antagonist on intravenous nicotine self administration and reinstatement of nicotine seeking. *PLoS ONE*. 2012;7:e29900.
- Grenald SA, Young MA, Wang Y, Ossipov MH, Ibrahim MM, Largent-Milnes TM, et al. Synergistic attenuation of chronic pain using mu opioid and cannabinoid receptor 2 agonists. *Neuropharmacology*. 2017;116:59–70.
- Zhang M, Dong L, Zou H, Li J, Li Q, Wang G, et al. Effects of cannabinoid type 2 receptor agonist AM1241 on morphine-induced antinociception, acute and chronic tolerance, and dependence in mice. *J Pain*. 2018;19:1113–29.
- Li AL, Lin X, Dhopeswarkar AS, Thomaz AC, Carey LM, Liu Y, et al. Cannabinoid CB2 agonist AM1710 awal. *Mol Pharmacol*. 2019;95:155–68.

36. Guenther KG, Wirt JL, Oliva I, Saberi SA, Crystal JD, Hohmann AG. The cannabinoid CB(2) agonist LY2828360 suppresses neuropathic pain behavior and attenuates morphine tolerance and conditioned place preference in rats. *Neuropharmacology*. 2025;265:110257.
37. Lin X, Dhopeswarkar AS, Huijbrete M, Mackie K, Hohmann AG. Slowly signaling G protein-biased CB(2) cannabinoid receptor agonist LY2828360 suppresses neuropathic pain with sustained efficacy and attenuates morphine tolerance and dependence. *Mol Pharmacol*. 2018;93:49–62.
38. Li X, Hua T, Vemuri K, Ho JH, Wu Y, Wu L, et al. Crystal structure of the human cannabinoid receptor CB2. *Cell*. 2019;176:459–67.e413.
39. Yeliseev A, Iyer MR, Joseph TT, Coffey NJ, Cinar R, Zoubak L, et al. Cholesterol as a modulator of cannabinoid receptor CB(2) signaling. *Sci Rep*. 2021;11:3706.
40. Hempel B, Xi ZX. Receptor mechanisms underlying the CNS effects of cannabinoids: CB(1) receptor and beyond. *Adv Pharmacol*. 2022;93:275–333.
41. Zhang HY, Shen H, Gao M, Ma Z, Hempel BJ, Bi GH, et al. Cannabinoid CB(2) receptors are expressed in glutamate neurons in the red nucleus and functionally modulate motor behavior in mice. *Neuropharmacology*. 2021;189:108538.
42. Stempel AV, Stumpf A, Zhang HY, Ozdogan T, Pannasch U, Theis AK, et al. Cannabinoid type 2 receptors mediate a cell type-specific plasticity in the hippocampus. *Neuron*. 2016;90:795–809.
43. Li Y, Kim J. Deletion of CB2 cannabinoid receptors reduces synaptic transmission and long-term potentiation in the mouse hippocampus. *Hippocampus*. 2016;26:275–81.
44. Schmöle AC, Lundt R, Gennequin B, Schrage H, Beins E, Kramer A, et al. Expression analysis of CB2-GFP BAC transgenic mice. *PLoS One*. 2015;10:e0138986.
45. Lopez A, Aparicio N, Pazos MR, Grande MT, Barreda-Manso MA, Benito-Cuesta I, et al. Cannabinoid CB(2) receptors in the mouse brain: relevance for Alzheimer's disease. *J Neuroinflammation*. 2018;15:158.
46. He XH, Jordan CJ, Vemuri K, Bi GH, Zhan J, Gardner EL, et al. Cannabinoid CB(1) receptor neutral antagonist AM4113 inhibits heroin self-administration without depressive side effects in rats. *Acta Pharmacol Sin*. 2019;40:365–73.
47. Xi ZX, Spiller K, Pak AC, Gilbert J, Dillon C, Li X, et al. Cannabinoid CB1 receptor antagonists attenuate cocaine's rewarding effects: experiments with self-administration and brain-stimulation reward in rats. *Neuropsychopharmacology*. 2008;33:1735–45.
48. Holtman JR Jr., Wala EP. Characterization of the antinociceptive effect of oxycodone in male and female rats. *Pharmacol Biochem Behav*. 2006;83:100–8.
49. Collins D, Reed B, Zhang Y, Kreek MJ. Sex differences in responsiveness to the prescription opioid oxycodone in mice. *Pharmacol Biochem Behav*. 2016;148:99–105.
50. Zhang HY, Gao M, Liu QR, Bi GH, Li X, Yang HJ, et al. Cannabinoid CB2 receptors modulate midbrain dopamine neuronal activity and dopamine-related behavior in mice. *Proc Natl Acad Sci USA*. 2014;111:E5007–5015.
51. Illum L. Nasal drug delivery: new developments and strategies. *Drug Discov Today*. 2002;7:1184–9.
52. Van Sickle MD, Duncan M, Kingsley PJ, Mouihate A, Urbani P, Mackie K, et al. Identification and functional characterization of brainstem cannabinoid CB2 receptors. *Science*. 2005;310:329–32.
53. Li Y, Kim J. Neuronal expression of CB2 cannabinoid receptor mRNAs in the mouse hippocampus. *Neuroscience*. 2015;311:253–67.
54. Zhang HY, Gao M, Shen H, Bi GH, Yang HJ, Liu QR, et al. Expression of functional cannabinoid CB(2) receptor in VTA dopamine neurons in rats. *Addict Biol*. 2017;22:752–65.
55. Navarrete F, Garcia-Gutierrez MS, Gasparyan A, Navarro D, Manzanares J. CB2 receptor involvement in the treatment of substance use disorders. *Biomolecules*. 2021;11:1556.
56. Cabanero D, Martin-Garcia E, Maldonado R. The CB2 cannabinoid receptor as a therapeutic target in the central nervous system. *Expert Opin Ther Targets*. 2021;25:659–76.
57. Lopes JB, Bastos JR, Costa RB, Aguiar DC, Moreira FA. The roles of cannabinoid CB1 and CB2 receptors in cocaine-induced behavioral sensitization and conditioned place preference in mice. *Psychopharmacology*. 2020;237:385–94.
58. Navarrete F, Garcia-Gutierrez MS, Manzanares J. Pharmacological regulation of cannabinoid CB2 receptor modulates the reinforcing and motivational actions of ethanol. *Biochem Pharmacol*. 2018;157:227–34.
59. Li J, Wang H, Liu D, Li X, He L, Pan J, et al. CB2R activation ameliorates late adolescent chronic alcohol exposure-induced anxiety-like behaviors during withdrawal by preventing morphological changes and suppressing NLRP3 inflammasome activation in prefrontal cortex microglia in mice. *Brain Behav Immun*. 2023;110:60–79.
60. Canseco-Alba A, Schanz N, Sanabria B, Zhao J, Lin Z, Liu QR, et al. Behavioral effects of psychostimulants in mutant mice with cell-type specific deletion of CB2 cannabinoid receptors in dopamine neurons. *Behav Brain Res*. 2019;360:286–97.
61. Ortega-Alvaro A, Ternianov A, Aracil-Fernandez A, Navarrete F, Garcia-Gutierrez MS, Manzanares J. Role of cannabinoid CB2 receptor in the reinforcing actions of ethanol. *Addict Biol*. 2015;20:43–55.
62. Dirik S, Doyle MR, Wood CP, Campo P, Martinez AR, Fannon M, et al. Cannabidiol mitigates alcohol dependence and withdrawal with neuroprotective effects in the basolateral amygdala and striatum. *Neuropsychopharmacology*. 2025.
63. Pertwee RG. The diverse CB1 and CB2 receptor pharmacology of three plant cannabinoids: delta9-tetrahydrocannabinol, cannabidiol and delta9-tetrahydrocannabinol. *Br J Pharmacol*. 2008;153:199–215.
64. Iyer V, Slivicki RA, Thomaz AC, Crystal JD, Mackie K, Hohmann AG. The cannabinoid CB(2) receptor agonist LY2828360 synergizes with morphine to suppress neuropathic nociception and attenuates morphine reward and physical dependence. *Eur J Pharmacol*. 2020;886:173544.
65. Galaj E, Bi GH, Xi ZX. beta-caryophyllene inhibits heroin self-administration, but does not alter opioid-induced antinociception in rodents. *Neuropharmacology*. 2024;252:109947.
66. Carey LM, Xu Z, Rajic G, Makriyannis A, Romero J, Hillard C, et al. Peripheral sensory neuron CB2 cannabinoid receptors are necessary for both CB2-mediated antinociceptive efficacy and sparing of morphine tolerance in a mouse model of anti-retroviral toxic neuropathy. *Pharmacol Res*. 2023;187:106560.
67. Zhang HY, Bi GH, Li X, Li J, Qu H, Zhang SJ, et al. Species differences in cannabinoid receptor 2 and receptor responses to cocaine self-administration in mice and rats. *Neuropsychopharmacology*. 2015;40:1037–51.
68. Liu QR, Pan CH, Hishimoto A, Li CY, Xi ZX, Llorente-Berzal A, et al. Species differences in cannabinoid receptor 2 (CNR2 gene): identification of novel human and rodent CB2 isoforms, differential tissue expression and regulation by cannabinoid receptor ligands. *Genes Brain Behav*. 2009;8:519–30.
69. Atwood BK, Mackie K. CB2: a cannabinoid receptor with an identity crisis. *Br J Pharmacol*. 2010;160:467–79.
70. Zhang HY, De Biase L, Chandra R, Shen H, Liu QR, Gardner E, et al. Repeated cocaine administration upregulates CB(2) receptor expression in striatal medium-spiny neurons that express dopamine D(1) receptors in mice. *Acta Pharmacol Sin*. 2022;43:876–88.
71. Guenther KG, Hohmann AG. Cannabinoid CB(2) receptor-mediated analgesia: mechanism-based insights and therapeutic potential. *Br J Pharmacol*. 2025.
72. Zhang M, Wang K, Ma M, Tian S, Wei N, Wang G. Low-Dose Cannabinoid Type 2 receptor agonist attenuates tolerance to repeated morphine administration via regulating mu-opioid receptor expression in Walker 256 tumor-bearing rats. *Anesth Analg*. 2016;122:1031–7.
73. Munro S, Thomas KL, Abu-Shaar M. Molecular characterization of a peripheral receptor for cannabinoids. *Nature*. 1993;365:61–65.
74. Brown SM, Wager-Miller J, Mackie K. Cloning and molecular characterization of the rat CB2 cannabinoid receptor. *Biochim Biophys Acta*. 2002;1576:255–64.
75. Schatz AR, Lee M, Condie RB, Pulaski JT, Kaminski NE. Cannabinoid receptors CB1 and CB2: a characterization of expression and adenylate cyclase modulation within the immune system. *Toxicol Appl Pharmacol*. 1997;142:278–87.
76. Li Y, Kim J. Distinct roles of neuronal and microglial CB2 cannabinoid receptors in the mouse hippocampus. *Neuroscience*. 2017;363:11–25.
77. Leppke K, Das R, Barna M. Functional 5' UTR mRNA structures in eukaryotic translation regulation and how to find them. *Nat Rev Mol Cell Biol*. 2018;19:158–74.

ACKNOWLEDGEMENTS

This research was supported by the Intramural Research Program of the National Institutes of Health (NIH) to Z.-X.X. (ZIA-DA000633) and M.R.I. (ZIA AA000360). The contributions of the NIH author(s) were made as part of their official duties as NIH federal employees, are in compliance with agency policy requirements, and are considered Works of the United States Government. However, the findings and conclusions presented in this paper are those of the author(s) and do not necessarily reflect the views of the NIH or the U.S. Department of Health and Human Services.

AUTHOR CONTRIBUTIONS

OSC, MRI, and Z-XX designed the experiments. EX, GHB, HA, and MM ran the behavioral experiments. HYZ carried out GFP IHC. Q-RL and Z-XX designed the CB2-KO-eGFP transgenic mouse line. PB and MRI provided both MRI-2594 and MRI-2687. OSC and X-ZX analyzed the data and finalized figures. OSC wrote a preliminary draft of the manuscript. Z-XX substantially revised and finalized the manuscript, incorporating feedback from all coauthors. All authors approved the final version of the manuscript for publication.

FUNDING

Open access funding provided by the National Institutes of Health.

COMPETING INTERESTS

The authors declare no competing interests.

ETHICS APPROVAL

All animal studies and experimental procedures (Animal Study Protocols 24-BNRR-48 and 25-BNRR-84) were approved by the Animal Care and Use Committee of the National Institute on Drug Abuse (NIDA), National Institutes of Health (NIH), U.S.A. All methods were carried out in accordance with the *Guide for the Care and Use of Laboratory Animals* (8th Edition, 2011). No human subjects or human samples were involved in this study.

ADDITIONAL INFORMATION

Supplementary information The online version contains supplementary material available at <https://doi.org/10.1038/s41380-025-03377-3>.

Correspondence and requests for materials should be addressed to Zheng-Xiong Xi.

Reprints and permission information is available at <http://www.nature.com/reprints>

Publisher's note Springer Nature remains neutral with regard to jurisdictional claims in published maps and institutional affiliations.



Open Access This article is licensed under a Creative Commons Attribution 4.0 International License, which permits use, sharing, adaptation, distribution and reproduction in any medium or format, as long as you give appropriate credit to the original author(s) and the source, provide a link to the Creative Commons licence, and indicate if changes were made. The images or other third party material in this article are included in the article's Creative Commons licence, unless indicated otherwise in a credit line to the material. If material is not included in the article's Creative Commons licence and your intended use is not permitted by statutory regulation or exceeds the permitted use, you will need to obtain permission directly from the copyright holder. To view a copy of this licence, visit <http://creativecommons.org/licenses/by/4.0/>.

This is a U.S. Government work and not under copyright protection in the US; foreign copyright protection may apply 2025